Modeling of Solid-Side Mass Transfer In Desiccant Particle Beds

Ahmad A. Pesaran (Solar Energy Research Institute)
Anthony F. Mills (University of Aukland)

February 1984

To be presented at the
ASME Sixth Solar Energy Divisional Conference
Las Vegas, Nevada
8-12 April 1984

ABSTRACT

A model is proposed for heat and mass transfer in a packed bed of desiccant particles and accounts for both Knudsen and surface diffusion within the particles. Using the model, predictions are made for the response of thin beds of silica gel particles to a step change in air inlet conditions and compared to experimental results. The predictions are found to be satisfactory and, in general, superior to those of pseudo-gas-side controlled models commonly used for the design of desiccant dehumidifiers for solar air conditioning application.

NOMENCLATURE

A — cross section area of bed (m^2)

c_b — specific heat of bed (J/kg K)

$c_{p,e}$ — constant pressure specific heat of humid air (J/kg K)

c_{pl} — constant pressure specific heat of water vapor (J/kg K)

DAR — desiccant to air ratio, $\rho_b AL/\dot{m}_G$ (dimensionless)

D — total diffusivity, defined by Eq. 9 (m^2/s)

D_K — Knudsen diffusion coefficient (m^2/s)

D_S — surface diffusion coefficient (m^2/s)

f, g — equilibrium isotherm

$g'(W)$ — derivative of equilibrium isotherm,

$$g'(W) = \left(\frac{\partial \rho m_1}{\partial W}\right)_T$$

h — enthalpy (J/kg)

h_1 — enthalpy of water vapor (J/kg)

h_c — convective heat transfer coefficient $(W/m^2 K)$

H_{ads} — heat of adsorption (J/kg water)

K_G — gas-side mass transfer coefficient $(kg/m^2 s)$

$K_{G,eff}$ — effective mass transfer coefficient $(kg/m^2 s)$

L — length of bed (m)

m_1 — water vapor mass fraction (kg water/kg moist air)

$\dot{m}_G$ — mass flow rate of gas mixture (kg/s)

n_1 — mass flux of H_2O $(kg/m^2 s)$

N_{tu} — number of transfer units, $K_G pL/\dot{m}_G$ (dimensionless)

P — pressure (kPa)

p — perimeter of bed (m)

PGC — pseudo-gas-side controlled

r — radial coordinate in a particle (m)

R — particle radius (m)

Re — Reynolds number, $2RV/\nu$ (dimensionless)

RH — relative humidity (dimensionless)

SSR — solid-side resistance

t — time (s)

t^* — t/τ (dimensionless)

T — temperature (^oC)

V — superficial velocity (m/s)

W — desiccant water content (kg water/kg dry desiccant)

z — axial distance (m)

Greek Symbols

ε_p — particle porosity (dimensionless)

ν — kinematic viscosity (m^2/s)

ρ — density (kg/m^3)

τ — duration of an experimental run (s)

τ_g — tortuosity factor for intraparticle gas diffusion (dimensionless)

τ_s — tortuosity factor for intraparticle surface diffusion (dimensionless)

Subscripts

l	water vapor
avg	average value
b	bed; bulk
e	external value
eff	effective value
in	inlet value
o	initial value
out	outlet value
p	particle
s	s-surface, in gas phase adjacent to gel particles

1. INTRODUCTION

Residential air conditioning comprises a considerable fraction of the total demand for electricity in the United States. Solar air conditioning has many advantages, such as reducing peak power requirements (peak load shaving) and efficient use of solar energy. Solar air conditioning systems that have received considerable attention in the last few years are solar-desiccant cooling systems. In many parts of the country a simple evaporative cooling system cannot give the desired air temperature without also producing excessive relative humidity levels (1).

The desiccant cooling system adds a desiccant unit to dry the humid air, and, in solar desiccant cooling systems, hot air from a solar air collector can be used to regenerate the desiccant. Thus, the only significant electrical power required by the solar desiccant cooling system is that used by the air fans. Both solid and liquid desiccants can be used. A suitable solid desiccant for solar desiccant cooling systems has been shown to be silica gel (2), because of its high moisture recycling capacity in the temperature range available. In order to meet system pressure drop constraints, thin desiccant beds must be used, and the quasi-steady breakthrough methods used to design thick industrial beds are not applicable. The transient response of thin silica gel packed beds is the concern of this study.

In general, adsorption of water vapor from air by a desiccant involves a number of physical processes, giving rise to resistances to vapor transfer from the gas phase to the solid phase. There is a gas-side resistance associated with transfer of vapor from the bulk gas to the adsorbent particle exterior surface, a solid-side resistance associated with diffusion of vapor or adsorbed molecules along the pores, and a kinetic or surface resistance associated with the adsorption process itself. Often one of these resistances is dominant, though more often at least two are important. Current practice is to analyze the dynamic performance of thin desiccant packed beds assuming a uniform particle moisture content and temperature and to model the overall transfer processes using pseudo-gas-side transfer coefficients (2,3,4,5).

Most often used has been the correlation of pseudo-gas-side transfer coefficients formulated by Hougen and Marshall (6), based on experimental data obtained by Ahlberg (7). Bullock and Threlkeld (4) were the first to numerically solve the partial differential equations governing mass and energy conservation in packed beds of silica gel particles. Pseudo-gas-side controlled processes were assumed, and the Hougen and Marshall correlation used. Calculations were made for thick beds typical of industrial applications. Nienberg (2) followed the approach of Bullock and Threlkeld and investigated the performance of thin beds for solar air conditioning application. His work was continued by Clark (3,8), and similar work was performed by Pla-Barby and Vliet (5). The pseudo-gas-side controlled model has also been used in analysis of desiccant bed performance by Mclaine-cross and Banks (9) and by Barlow (10).

Clark (3,8) tested a prototype scale stationary bed designed for solar air conditioning application and found poor agreement between analytical prediction and experiment for the instantaneous outlet air humidity and temperature, particularly after a step change in inlet condition. Although there was some doubt as to the most suitable equilibrium vapor pressure and heat of adsorption data, Clark concluded that the discrepancy was mainly due to improper treatment of solid-side mass transfer resistance in the model, especially at high temperatures and low desiccant moisture contents. Pesaran (11) performed extensive bench scale experiments on thin packed beds of Regular Density (RD) silica gel with a step change in inlet humidity. He compared his results with predictions of an improved version of Nienberg's computer code (2) and concluded that the solid-side resistance was possibly greater than the gas-side resistance, and the use of a pseudo-gas-side resistance in analytical models was inappropriate. Based on a survey of the available literature on mass transfer in packed beds he suggested appropriate correlations for the actual gas-side transfer coefficients for desiccant packed beds.

The purpose of the present work was to develop a model for heat and mass transfer in silica gel packed particle beds that properly accounts for solid-side diffusion. The theoretical model was formulated using available information about the nature of diffusion of water in silica gel, the undetermined constants evaluated through comparison of predictions using the model, and experimental data obtained for the transient response of thin packed beds at parameter values characteristic of solar air conditioning application.

2. MODELING AND ANALYSIS

The overall strategy was to first develop a general equation for moisture transport in an isothermal spherical desiccant particle and then to incorporate this equation into the equation set governing heat and mass transfer in a packed particle bed.

At atmospheric pressure, and for the pore radii characteristic of silica gel, ordinary diffusion of moisture may be ignored, and only the mechanisms of Knudsen and surface diffusion need be considered (12). Figure 1 shows a spherical silica gel particle for which the equation governing conservation of moisture is

$$\varepsilon_p \frac{\partial(\rho m_1)}{\partial t} + \rho_p \frac{\partial W}{\partial t} = -\frac{1}{r^2}\frac{\partial}{\partial r}(r^2 n_1). \tag{1}$$

Since Knudsen and surface diffusion are parallel processes, they are additive if interactions are ignored, thus

$$n_1 = -\rho_p D_{S,eff}\frac{\partial W}{\partial r} - \rho D_{K,eff}\frac{\partial m_1}{\partial r}. \tag{2}$$

The initial conditions are

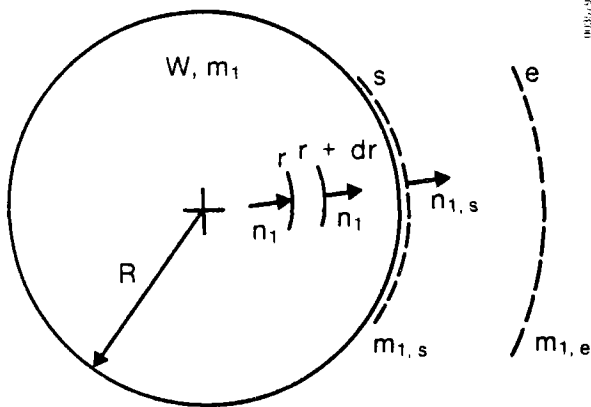$$W(r,t=0) = W_o(r) \ ; \ \rho m_1(r,t=0) = \rho_o m_{1o}(r), \tag{3a,b}$$

$$\frac{\partial W}{\partial t} = \frac{1}{r^2} \frac{\partial}{\partial r} \left[r^2 D \frac{\partial W}{\partial r} \right]; \qquad (10)$$

I.C.: $\qquad W(r, t=0) = W_o(r); \qquad (11)$

B.C.'s: $\qquad \left. \frac{\partial W}{\partial r} \right|_{r=0} = 0 \qquad (12)$

$$-\rho_p D \left. \frac{\partial W}{\partial r} \right|_{r=R} = K_G(m_{1,s} - m_{1,e}) ; \quad (13)$$

coupling condition:

$$m_{1,s}(t) = f[W(r=R,t),T,P] . \qquad (14)$$

The ratio of Knudsen to surface diffusion fluxes in a desiccant particle is

$$\frac{n_{1,K}}{n_{1,S}} = \frac{D_{K,eff}}{D_{S,eff}} \frac{g'(W)/\rho_p}{} , \qquad (15)$$

which depends on the average pore radius, internal particle structure, the equilibrium isotherm slope, and temperature. This ratio was calculated for both Regular Density (RD) and Intermediate Density (ID) gels (12). The calculations show that the dominant mechanism in RD gel (average pore radius 11 Å) is surface diffusion, while both surface and Knudsen diffusion should be considered for ID gel (average pore radius 68 Å).

The differential equations governing the transient response of a packed bed of desiccant particles is next presented. These equations are obtained by applying the principles of mass, species, and energy conservation in both phases. Figure 2 shows an idealized picture of the physical phenomena in the gas phase. It can be shown that gas-side storage terms $\partial m_{1,e}/\partial t$ and $\partial T_e/\partial t$ are negligible compared to the other terms for thin beds. Axial and radial diffusion and conduction are ignored. The bed is assumed to be adiabatic. Assuming isothermal particles, a "lumped-capacitance" model can be used for energy conservation in the solid phase. With these assumptions the governing equations are:

species conservation in the gas-phase

$$\dot{m}_G \frac{\partial m_{1,e}}{\partial z} = K_G(m_{1,s} - m_{1,e})(1 - m_{1,e})p , \quad (16)$$

species conservation in the solid-phase

$$\frac{\partial W}{\partial t} = \frac{1}{r^2} \frac{\partial}{\partial r} \left(D r^2 \frac{\partial W}{\partial r} \right) , \qquad (17)$$

energy conservation in the solid-phase

$$A \rho_b c_b \frac{\partial T_s}{\partial t} = p[h_c(T_e - T_s) - H_{ads} K_G(m_{1,s} - m_{1,e})] , \quad (18)$$

and energy conservation in the gas-phase

$$c_{p,e} \dot{m}_G \frac{\partial T_e}{\partial z} = - p[h_c + c_{p1} K_G(m_{1,s} - m_{1,e})](T_e - T_s) . \quad (19)$$

The details of the development of the above equations can be found in Pesaran (12). The equations are coupled through the equilibrium relation applied at the particle surface,

$$m_{1,s}(z,t) = f[W(r=R,z,t),T_s(z,t),P] ; \quad (20)$$

and the initial and boundary conditions for the equations are

I.C.1 $\qquad W(r,z,t=0) = W_o(r,z) \qquad (21)$

Fig. 1. Diffusion Through a Spherical Particle

while the boundary conditions are

zero flux at $r = 0$; $\left. n_1 \right|_{r=0} = 0$; $\qquad (4)$

and

flux continuity at $r = R$; $\left. n_1 \right|_{r=R} = K_G(m_{1,s} - m_{1,e})$. $\quad (5)$

Also m_1 and W are related through the equilibrium relation

$$\rho m_1(r,t) = g[W(r,t),T] , \qquad (6)$$

while continuity of gas phase concentration requires

$$\left. m_1 \right|_{r=R} = m_{1,s}(t) . \qquad (7)$$

By setting either $D_{S,eff}$ or $D_{K,eff}$ equal to zero the cases of dominant Knudsen diffusion or dominant surface diffusion can be obtained.

The problem can be further simplified if an isothermal particle is assumed. This assumption is reasonable since for most of the range of air conditioning applications the Biot number of the particles is less than 0.15 (12). The number of the unknowns can then be reduced by eliminating ρm_1 using the equilibrium relation Eq. (6). Using the chain rule of differentiation and after some manipulation, Eqs. (1) and (2) become

$$\frac{\partial W}{\partial t} = \frac{1}{\left(\frac{\epsilon_p g'(W)}{\rho_p} + 1 \right)} \frac{1}{r^2} \frac{\partial}{\partial r} \left(r^2 [D_{S,eff} \right.$$
$$\left. + D_{K,eff} \frac{g'(W)}{\rho_p} \right] \frac{\partial W}{\partial r} \right) , \qquad (8)$$

where

$$g'(W) = \left(\frac{\partial(\rho m_1)}{\partial W} \right)_T .$$

The value of $\epsilon_p g'(W)/\rho_p$ is usually much less than unity for most desiccants and will be ignored (12). Physically this corresponds to neglecting the gas storage term $\epsilon_p (\partial \rho m_1/\partial t)$ in Eq. (1). If we now define a total diffusivity D, we see that

$$D = D_{S,eff} + D_{K,eff} \frac{g'(W)}{\rho_p} . \qquad (9)$$

Equations (3) through (8) become

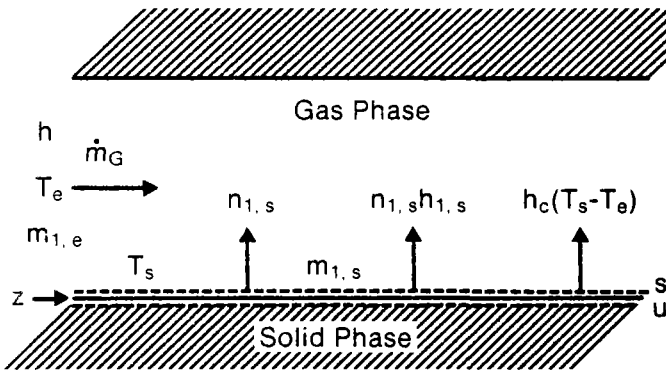**Fig. 2. Idealized Picture of the Physical Phenomena in the Gas Phase**

I.C.2 $\quad T_s(z,t=0) = T_0(z)$ (22)

B.C.1 $\quad \left.\dfrac{\partial W}{\partial r}\right|_{r=0} = 0$ (23)

B.C.2 $\quad -\rho_p D \left.\dfrac{\partial W}{\partial r}\right|_{r=R} = K_G[m_{1,s}(z,t) - m_{1,e}(z,t)]$ (24)

B.C.3 $\quad m_{1,e}(z=0,t) = m_{1,in}(t)$ (25)

B.C.4 $\quad T_e(z=0,t) = T_{in}(t)$. (26)

In the evaluation of the heat of the adsorption H_{ads} and specific heat of the moist desiccant c_b an average desiccant moisture content is required, which is

$$W_{avg} = \dfrac{\displaystyle\int_0^R 4\pi r^2 W \rho_p \, dr}{\tfrac{4}{3}\pi R^3 \rho_p} .$$ (27)

Equations (16) through (27) are a complete set of coupled nonlinear partial differential equations and boundary and initial conditions with six unknowns: $W(r,z,t)$, $W_{avg}(z,t)$, $m_{1,s}(z,tu4$ $B_{1,e}(z,t)$, $T_s(z,t)$, $T_e(z,t)$.

If the mass transfer problem is treated as a lumped-capacitance model, as has been done by investigators using pseudo-gas-side controlled models [e.g., (2,4,5)], the solid phase species conservation equation becomes

$$A\rho_b \dfrac{\partial W_{avg}}{\partial t} = K_{G,eff}(m_{1,s} - m_{1,e})p ,$$ (28)

where $K_{G,eff}$ is a psuedo-gas-side, mass transfer coefficient, given here by the Hougen and Marshall correlation.

The above equation set was put in dimensionless form and then solved numerically. The Crank-Nicholson scheme was used for Eq. (17), while the implicit Euler method was used for Eq. (18). A fourth-order Runge-Kutta technique was used for the spatial equations, Eqs. (16) and (19). Three nondimensional parameters are involved:

$$N_{tu} = \dfrac{K_G pL}{\dot{m}_G} \; ; \quad DAR = \dfrac{\rho_b AL}{\dot{m}_G \tau} \; ; \quad \beta = \dfrac{\rho_p D}{K_G R} .$$

3. EXPERIMENTAL APPROACH

3.1 Apparatus

The experimental system consisted of a dryer, an air heater, a humidifier, a blower, and a desiccant bed in a test chamber. The dryer and the humidifier were used to generate the desired inlet air conditions (temperature and humidity) for the test chamber, the air heater was used to regenerate the desiccant both in the test chamber and the dryer. The dryer was a packed bed of Davison 03 silica gel, while the humidifier consisted of Berl saddle packing and overhead water spray. The desiccant bed in a 0.13 m ID cylinder was supported by a copper screen. The height of the bed was varied by adding more or less desiccant. To approximate the adiabatic situation, the test chamber was insulated with fiberglass in the vicinity of the desiccant bed during testing.

3.2 Instrumentation

The pressure drop across the bed was measured using a water manometer. The air temperature upstream and downstream of the bed, humidifier, and dryer were measured using thermocouples made from 30-gauge, chromel-alumel wires. The relative humidity of the processed air was measured using a hygrometer manufactured by Weathermeasure Corp. with a single dielectric polymer sensor having a very short response time (90% relative humidity change in one second). The electrical signals of the thermocouples and hygrometers were recorded simultaneously at a pre-programmed time interval.

3.3 Procedure

Tests were performed to determine the response of a bed to a step change in inlet air conditions. A bed of known initial water content and temperature was prepared using the heater, the humidifier, or the dryer, and then at time $t = 0$, process air with selected constant humidity and temperature was passed through the bed. The outlet air conditions from the bed were measured and plotted versus time. Two types of experiments were performed, namely, adsorption and desorption. In adsorption experiments the initial bed water content was much lower than the equilibrium value corresponding to the process air, while in desorption experiments, the initial bed water content was much higher than the equilibrium value corresponding to the process air.

3.4 Test Gel

Both the RD gels (Davison Grade 01, 03, 40 and 408) and ID gel (Davison Grade 59) were tested to investigate the effect of average pore diameter and equilibrium adsorption on bed performance. Since it can reasonably be assumed that the solid-side resistance varies with desiccant particle size, a wide range of gel sizes was tested (0.6-5 mm). Different grades of silica gel were sieved to obtain a narrow range of particle size.

4. RESULTS AND DISCUSSION

The numerical solution of the diffusion equation for a single particle, Eq. (10), is discussed first. Next, predictions using the theoretical models of bed performance developed in Sec. 2 will be compared with the experimental data for RD and ID gels.

4.1 Numerical Solutions of the Diffusion Equation in an Isothermal Particle

The numerical solutions to the diffusion equation for an RD and an ID particle are presented in Figs. 3 and 4, respectively. The figures show the gel water

content as a function of time for adsorption cases of typical experimental conditions in the range of solar air conditioning. The result for an RD particle, Fig. 3, shows that the difference between curve 1 (surface plus Knudsen diffusion) and curve 2 (surface diffusion only) is very small, and thus confirms that the contribution of Knudsen diffusion can be neglected for RD gel.

Figure 4 shows that the contribution of Knudsen diffusion cannot be neglected for ID gel. Note that the curves of W_{avg} versus t^* for each mechanism cannot be simply added since the problem is a nonlinear one. Investigation of profiles of local gel water content shows that the penetration of water into ID particles is faster than that of RD particles, because the total diffusivity of ID gel is larger than that of RD gel (about 4-20 times greater). The auxiliary data such as heat of adsorption, equilibrium isotherm, surface diffusion coefficient, etc., are presented in Table 1.

4.2 Comparisons of Experimental Results with Theoretical Predictions

Table 2 summarizes the pertinent parameters of some of the successful experimental runs. Figures 5 through 12 show the outlet air temperature and water vapor mass fraction as a function of dimensionless time. Theoretical predictions using both the model with solid-side resistance (SSR model) and pseudo-gas-side controlled model (PGC model) are also shown in Figs. 5 through 12. The general trend of both theoretical and experimental adsorption results are as follows: T_{out} increases rapidly to a maximum and gradually decreases at a rate depending on the air flow
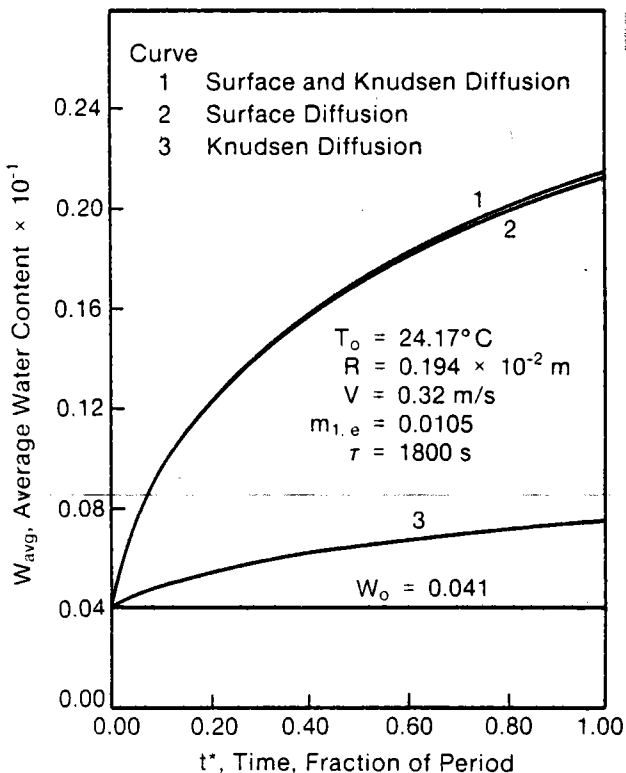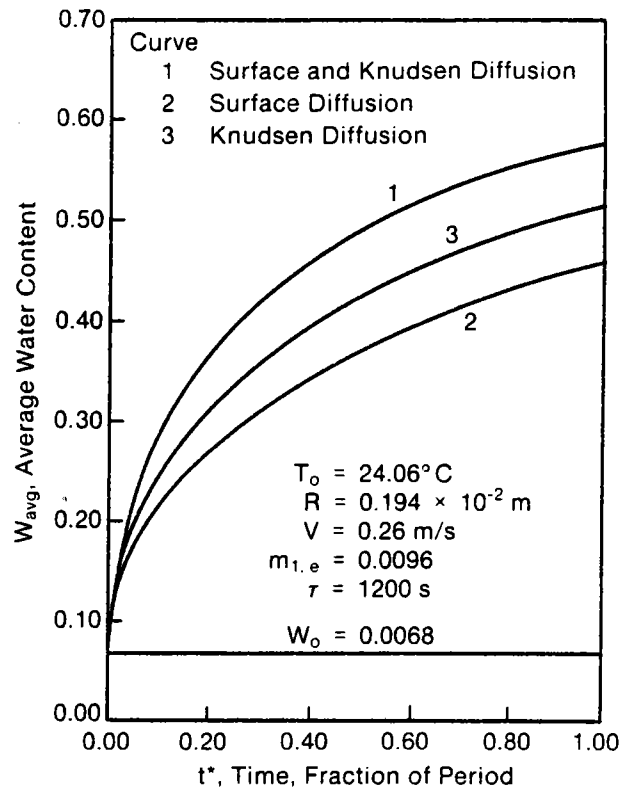
Fig. 4. W_{avg} vs. t^* for Various Mechanisms of Diffusion for an Intermediate Density Particle

rate; $m_{1,out}$ also increases rapidly at first, but rather than reaching a maximum, the rate of increase simply becomes less. The change in slope of $m_{1,out}$ occurs after T_{out} reaches its peak. The reasons for this behavior are that immediately following the step change, the dry bed adsorbs H_2O and liberates heat at a high rate; consequently, the bed temperature and T_{out} increase rapidly, and $m_{1,out}$ increases rapidly from a value much lower than $m_{1,in}$. The bed gradually loses its adsorptive capacity due to the increase in gel water content and bed temperature, and the rate of increase of $m_{1,out}$ decreases as a result. The maximum in T_{out} is reached when the cooling effect of the air flow balances the heat of adsorption being released, and thereafter the reduced rate of adsorption causes T_{out} to decrease.

Comparing the theories and experiments we observe the following. For adsorption on RD gel (Figs. 5, 6, 7, 12) agreement between the predictions of SSR model and experiments is good, being somewhat better for $m_{1,out}$ than T_{out}. The predictions of $m_{1,out}$ using the SSR model are generally better than those of the PGC model, especially at small times. The initial slope of the $m_{1,out}$ curve from SSR model is steeper than those of PGC model and is usually the same as the experimental value. For desorption from the RD gel (Figs. 10, 11) generally, $m_{1,out}$ is overpredicted by both models, while T_{out} is predicted satisfactorily by the SSR model and underpredicted by PGC model. The agreement between $m_{1,out}$ predictions of the models and experiments are not as good as those of adsorption cases. This behavior has also been observed elsewhere (10) and may be attributed to presence of a dynamic hysteresis in the adsorption/desorption characteristics of silica gel. For adsorption on ID gel

Fig. 3. W_{avg} vs. t^* for Various Mechanisms of Diffusion for a Regular Density Particle

Table 1. Auxiliary Data for Regular and Intermediate Density Silica Gels (12)

	Regular Density	Intermediate Density
Heat of adsorption	$H_{ads} = -12400W + 3500 \quad W < 0.05$ $H_{ads} = -1400W + 2950 \quad W > 0.05$	$H_{ads} = -300W + 2095 \quad W < 0.15$ $H_{ads} = 2050 \quad W > 0.15$
Equilibrium isotherm	$RH = 0.0078 - 0.05759W + 24.16554W^2$ $\quad - 124.478W^3 + 204.228W^4$	$RH = 1.235W + 267.9W^2 - 3170.7W^3$ $\quad + 10087.16W^4 \quad W < 0.07$ $RH = 3.18W + 0.348 \quad W > 0.07$
Tortuosity factor	$\tau_g = \tau_s = 2.8$	$\tau_g = \tau_s = 2$
Particle porosity	$\varepsilon_p = 0.516$	$\varepsilon_p = 0.716$
Bulk density	$\rho_b = 721.1 \text{ kg/m}^3$	$\rho_b = 400.6 \text{ kg/m}^3$
Particle density	$\rho_p = 1185.9 \text{ kg/m}^3$	$\rho_p = 620 \text{ kg/m}^3$
Gas-side mass transfer coefficient	$K_G = 1.70 \dfrac{\dot{m}G}{A} Re^{-0.42} \quad \text{kg/m}^2 s$	
Gas-side heat transfer coefficient	$h_c = 1.60 \dfrac{\dot{m}G}{A} Re^{-0.42} c_{p,e} \quad W/m^2 K$	
Surface diffusion coefficient	$D_S = D_o \exp[-0.974 H_{ads}/(T + 273)] \text{ m}^2/s$	
Knudsen diffusion coefficient	$D_K = 22.86a(T + 273)^{1/2} \quad \text{m}^2/s; \quad a = \text{average pore radius (m)}$	
Effective diffusion coefficients	$D_{K,eff} = \dfrac{\varepsilon_p}{\tau_g} D_K \qquad D_{S,eff} = \dfrac{1}{\tau_s} D_S$	

Table 2. Bed and Flow Conditions of the Experiments

Run	Gel Type	R $(10^{-3}$ m)	L $(10^{-2}$ m)	W_o	T_o (°C)	$m_{1,in}$	T_{in} (°C)	V (m/s)	Re	N_{tu}*	DAR	τ (s)
1	RD	1.94	7.75	0.0417	23.3	0.0100	23.3	0.21	49.3	22.65	0.1285	1800
3	RD	1.94	7.75	0.0415	21.6	0.0078	21.6	0.34	84.4	18.80	0.0812	1740
7	RD	1.27	6.5	0.0410	24.7	0.0106	24.7	0.39	70.0	26.90	0.0604	1800
13	ID	1.94	7.75	0.0088	23.6	0.0097	23.67	0.45	109.5	16.9	0.050	1200
17	ID	1.94	7.75	0.0050	24.44	0.0063	24.44	0.67	164.2	14.2	0.033	1200
27	RD	2.60	5.0	0.296	22.78	0.0007	22.78	0.30	94.5	8.71	0.0586	1800
28	RD	2.60	5.0	0.241	24.17	0.0005	24.17	0.42	133.2	7.54	0.0621	1200
31	RD	2.60	5.0	0.045	22.89	0.0158	22.83	0.25	79.4	9.36	0.0702	1800

*This value of N_{tu} is for the SSR model; N_{tu} for the PGC model is approximately 1/3.4 of this N_{tu}.

(Figs. 8, 9) the SSR model predicts $m_{1,out}$ well at small times, but overpredicts $m_{1,out}$ later. The predictions of the SSR model are better than those of the PGC model for $m_{1,out}$. T_{out} is generally underpredicted by both models, with the PGC model being somewhat better. These discrepancies can be attributed partly to the lack of reliable data for the adsorption isotherm and the heat of adsorption of the ID gel.

5. CONCLUDING REMARKS

A new model has been developed for heat and mass transfer in a packed bed of silica gel desiccant particles that properly accounts for both Knudsen and surface diffusion within the particles. Predictions of transient bed response agree quite well with experiments, and, in general, are somewhat better than predictions given by the commonly used pseudo-gas-side controlled model. Since the new model is more faithful to the true physics of the problem, it is likely that it can be used to extrapolate available experimental data with much greater confidence than can be done with existing pseudo-gas-side controlled models.
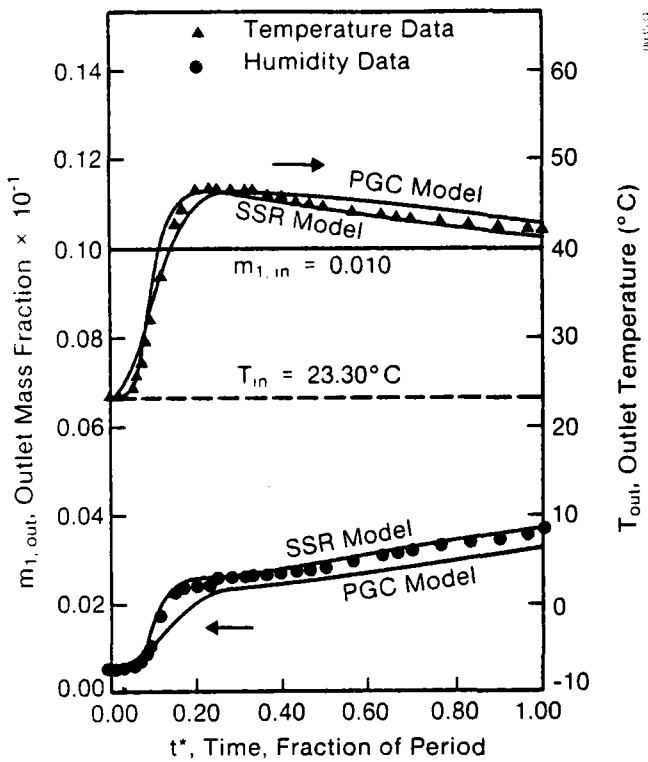
Fig. 5. Comparison of Experimental and Predicted Results for Run 1 (RD, Adsorption); $D_o = 4.48 \times 10^{-6} \text{ m}^2/\text{s}$
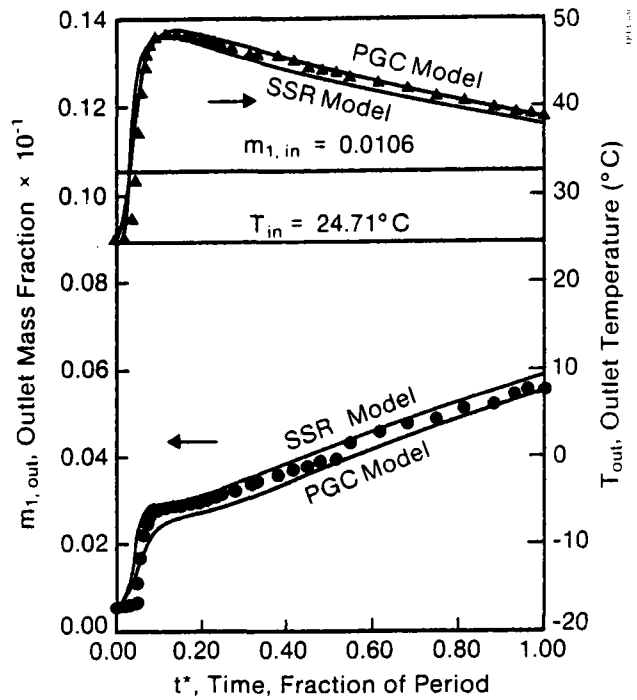
Fig. 7. Comparison of Experimental and Predicted Results for Run 7 (RD, Adsorption); $D_o = 4.48 \times 10^{-6} \text{ m}^2/\text{s}$
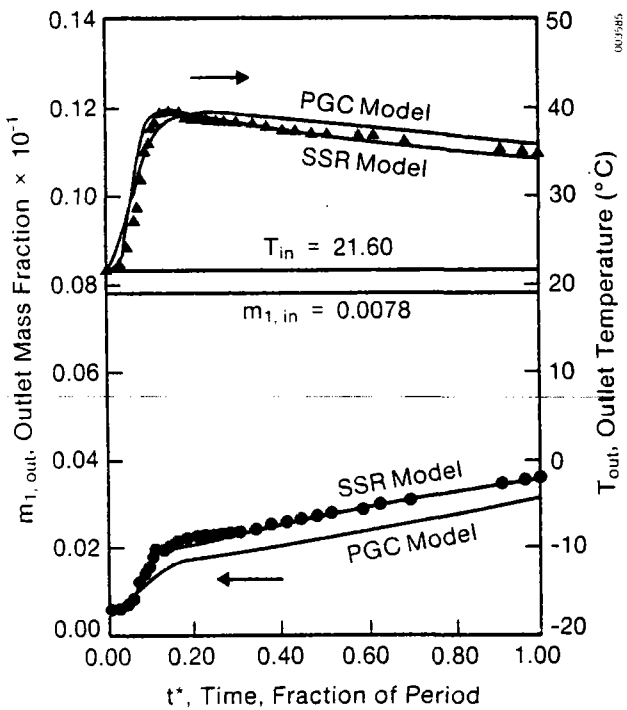
Fig. 6. Comparison of Experimental and Predicted Results for Run 3 (RD, Adsorption); $D_o = 4.48 \times 10^{-6} \text{ m}^2/\text{s}$
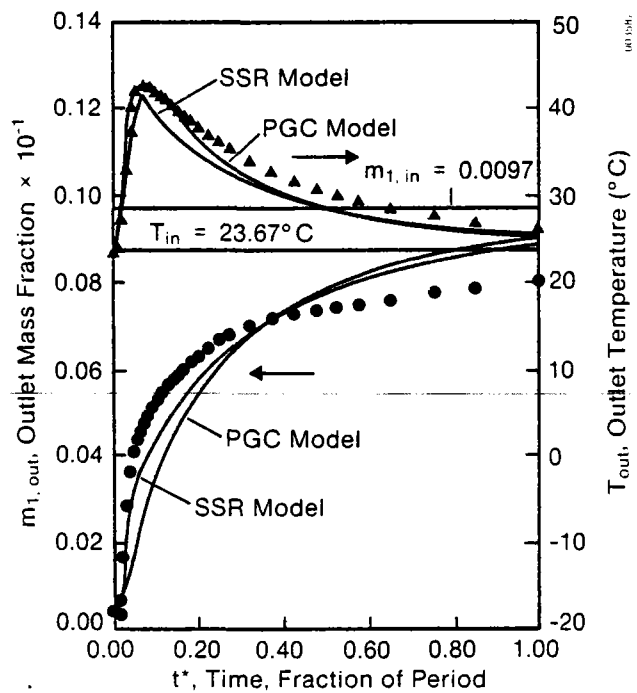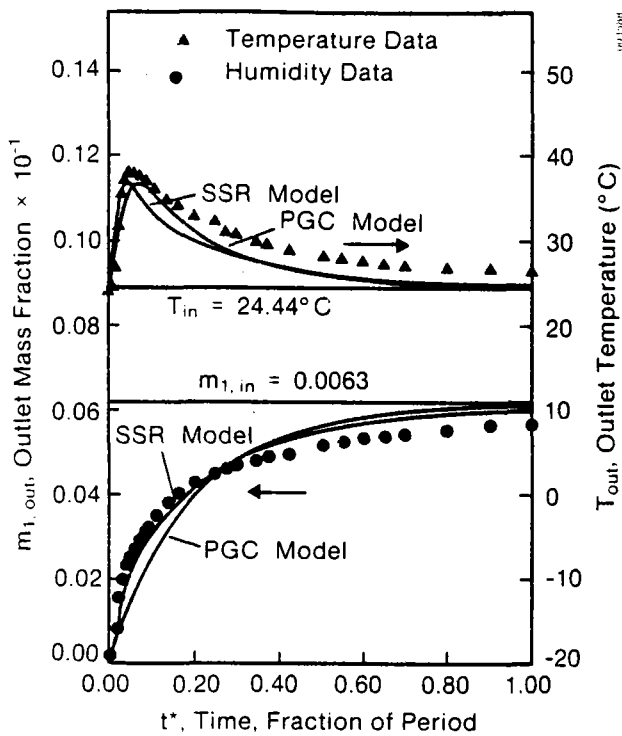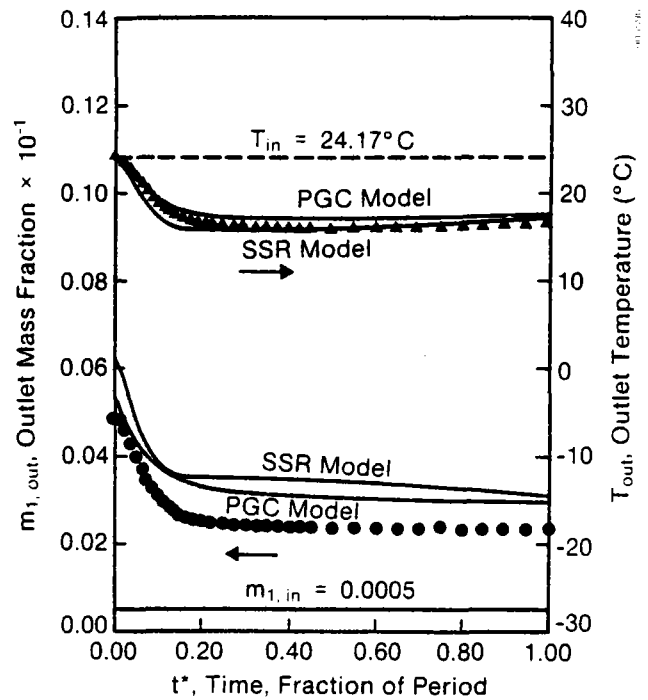
Fig. 8. Comparison of Experimental and Predicted Results for Run 13 (ID, Adsorption); $D_o = 3.2 \times 10^{-6} \text{ m}^2/\text{s}$
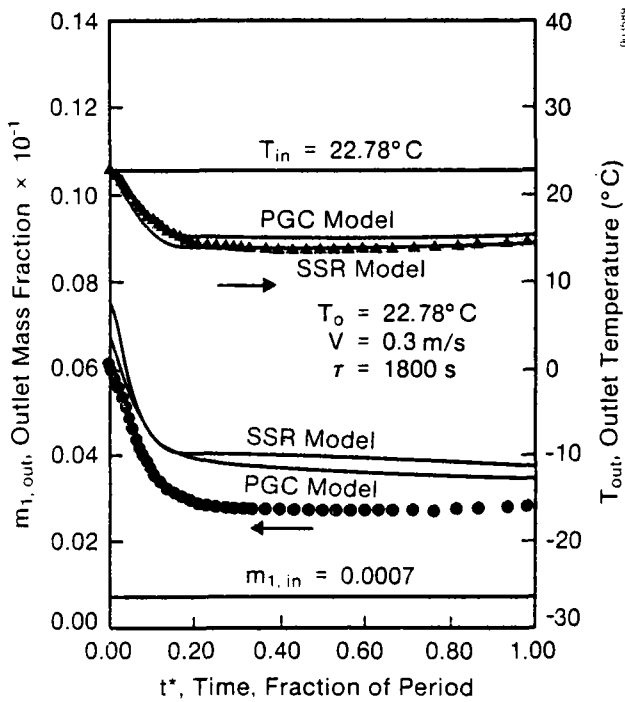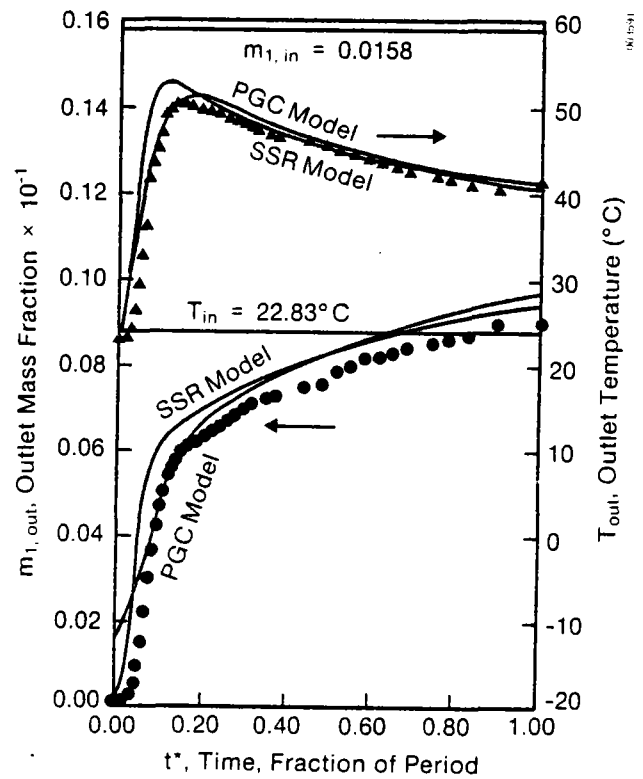
7

Fig. 9. Comparison of Experimental and Predicted Results for Run 17 (ID, Adsorption); $D_o = 3.2 \times 10^{-6}$ m^2/s

Fig. 11. Comparison of Experimental and Predicted Results for Run 28 (RD, Desorption); $D_o = 2.28 \times 10^{-6}$ m^2/s

Fig. 10. Comparison of Experimental and Predicted Results for Run 27 (RD, Desorption); $D_o = 2.28 \times 10^{-6}$ m^2/s

Fig. 12. Comparison of Experimental and Predicted Results for Run 31 (RD, Adsorption); $D_o = 4.48 \times 10^{-6}$ m^2/s

8

6. ACKNOWLEDGMENTS

7. REFERENCES

1. Buchberg, H., and Lassner, N., "Performance of an Experimental Regenerative-Evaporative Cooler Compared with Predictions," Proc. 1977 Int. Center Heat and Mass Transfer, Dubrovnik, Yugoslavia, Aug. 1977, Hemisphere Publishing Co.

2. Nienberg, J. W., "Modeling of Desiccant Performance for Solar-Desiccant-Evaporative Cooling Systems," M.S. Thesis, School of Engineering and Applied Science, University of California, Los Angeles, 1977.

3. Clark, J. W., Mills, A. F., and Buchberg, H., "Design and Testing of Thin Adiabatic Desiccant Beds for Solar Air Conditioning Applications," J. Solar Energy Engineering, Vol. 103, May 1981, pp. 89-91.

4. Bullock, C. E., and Threlkeld, J. L., "Dehumidification of Moist Air by Adiabatic Adsorption," Trans. ASHRAE, Vol. 72, part I, 1966, pp. 301-313.

5. Pla-Barby, F. E., and Vliet, G. C., "Rotary Bed Solid Desiccant Drying: An Analytical and Experimental Investigation," ASME/AIChE 18th National Heat Transfer Conference, San Diego, CA, Aug. 1979, (ASME paper 79-HT-19).

6. Hougen, O. A., and Marshall, W. R., Jr., "Adsorption from a Fluid Stream Flowing Through a Stationary Granular Bed," Chem. Eng. Prog., Vol. 43, No. 4, April 1947, pp. 1971-208.

7. Ahlberg, J. E., "Rates of Water Vapor Adsorption for Air by Silica Gel," Ind. Eng. Chem., No. 31, Aug. 1939, pp. 988-992.

8. Clark, J. E., "Design and Construction of Thin, Adiabatic Desiccant Beds with Solar Air Conditioning Applications," M.S. Thesis, School of Engineering and Applied Science, University of California, Los Angeles, 1979.

9. Maclaine-cross, I. L. and Banks, P. J., "Coupled Heat and Mass Transfer in Regenerators—Prediction Using an Analogy with Heat Transfer," Int. J. Heat Mass Transfer, Vol. 15, 1972, pp. 1225-1242.

10. Barlow, R. S., Analysis of Adsorption Process and of Desiccant Cooling Systems—A Pseudo-Steady-State Model for Coupled Heat and Mass Transfer," SERI/TR-631-1329, Dec. 1982, Solar Energy Research Institute, Golden, CO.

11. Pesaran, A. A., "Air Dehumidification in Packed Silica Gel Beds," M.S. Thesis, School of Engineering and Applied Science, University of California, Los Angeles, 1980.

12. Pesaran, A. A., "Moisture Transport in Silica Gel Particle Beds," Ph.D Dissertation, School of Engineering and Applied Science, University of California, Los Angeles, 1983.